

Polarimetric SAR Interferometry for Forest Canopy Analysis by Using the Super-resolution Method

H. Yamada¹, Y. Yamaguchi¹, E. Rodriguez², Y. Kim², W. M. Boerner³

1: Department of Information Engineering, Niigata University
Ikarashi 2-8050, Niigata 950-2181, JAPAN

Tel/Fax: +81-25-262-7477, e-mail: yamada@ie.niigata-u.ac.jp
2: Jet Propulsion Laboratory, California Institute of Technology
4800 Oak Grove Drive, Pasadena, CA 91109-8099, USA

3: University of Illinois at Chicago
UIC-EECS/CSN, m/c 154, SEL 4210
900 West Taylor Street, Chicago, IL/USA 60607-7018

Abstract—In this paper, we propose an polarimetric SAR interferometry technique for interferometric phase extraction of each local scatterer of the forest region. The proposed method formulated for local scattering center extraction is based on the ESPRIT algorithm which is known for high-resolution capability of closely located incidences. The method shows high-resolution performance when local scattered waves are uncorrelated and have different polarization characteristics. Using the method, the number of dominant local scattered waves and their interferometric phases in each image patch can be estimated directly. Validity of the algorithm is demonstrated by using examples derived from SIR-C data.

I. INTRODUCTION

Recently, many research studies have been proposed for biomass estimation using the interferometric approach [1]–[4]. The back-scattering waves resulting from the forest region can be expressed in terms of several parameters of ground and canopy scattering mechanisms. Therefore, multi-baseline and polarimetric techniques are required to acquire sufficient information for the parameter inversion [3], [4].

In this paper, we focus on the polarimetric technique. Polarization is sensitive to the shape, orientation, textural fine structure, and dielectric constant variations inside a canopy volume [5]. Therefore, polarimetry is one of the promising techniques for forest -versus- ground scattering estimation. Cloude and Papathannassou utilized these properties and realized *Polarimetric SAR Interferometry* based on the coherence optimization [4]. In addition, a parameter inversion technique [5], using the optimization technique, was also proposed by them. This technique is very attractive. However, this particular multiple inversion approach requires multi-parameter least-square estimation whose complexity is high, and often becomes ill-conditioned.

In this paper, we propose an alternate *Polarimetric SAR Interferometry* technique based on the ESPRIT (Estimation of Signal Parameters via Rotational Invariance Techniques) algorithm [6]. The ESPRIT algorithm is often employed for *Direction-of-Arrival* estimation for antenna arrays. We

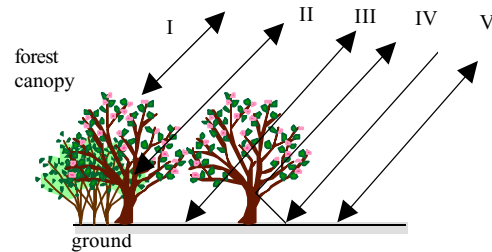


Fig.1 Local scattering mechanism of vegetated region

show, in this paper, that interferometric phases of the ground and canopy can be directly resolved by this algorithm. When these phases are estimated, the derivation of the remaining parameters of the forest canopy becomes less complicated.

II. CANOPY MODEL

For forest observations, the backscattered waves can be considered as the sum of the components shown in Fig.1 [5]. These components can be classified into two groups: the first one corresponds to the waves whose local scattering center is located in the forest canopy (I, II); and the other corresponds to the waves whose local scattering center is located approximately on the ground (III, IV, V). Therefore, the distribution of the effective scattering coefficient across the forested terrain can be approximately modeled in terms of these two components. Since the observed signals can be modeled in terms of these two components possessing different local scattering centers, the scattering centers estimated by the interferometric phase are located between the upper canopy layer and the ground; and the interferometric coherence decreases because the components, in Fig.1, are uncorrelated in general. In the ESPRIT applications, we utilize the uncorrelated property of local scattered waves in addition to their polarization differences.

III. THE ESPRIT ALGORITHM

For simplicity, we use {HV}-basis measurements of 3 channel data (HH, HV, and VV), and assume that there exist two scattering centers corresponding to the ground and forest,

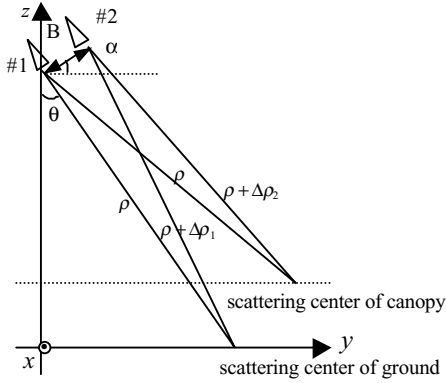


Fig.2 Interferometric SAR geometry

respectively. In this case, using the geometry of Fig.2, the observed signals in orbit-1 and in orbit-2 may be written as

$$E_1^{(kl)} = \sum_{i=1}^2 \sigma_i s_i^{(kl)} e^{j4\pi\rho/\lambda} + n_1^{(kl)}$$

$$E_2^{(kl)} = \sum_{i=1}^2 \sigma_i s_i^{(kl)} e^{j4\pi(\rho+\Delta\rho_i)/\lambda} + n_2^{(kl)}$$
(1)

where k, l denote polarization combinations (e.g. HH, HV, and VV). $s_i^{(kl)}$ denotes the polarization state of the i -th local scatterer in kl polarization. Each polarization state is assumed to be normalized with respect to the power of the local scatterer; σ_i denotes complex amplitude of the i -th scattered wave; ρ is the slant-range distance from the orbit-1 to the range bin; $\Delta\rho_i$ denotes the slant-range difference of the scatterer; and $n_1^{(kl)}$ and $n_2^{(kl)}$ denote the additive noise in kl channel at orbit-1 and orbit-2, respectively.

Using matrix-vector expressions, (1) can be written as

$$E_1 = [E_1^{(HH)}, E_1^{(HV)}, E_1^{(VV)}]^T = \mathbf{S}\boldsymbol{\sigma} + \mathbf{n}_1$$

$$E_2 = [E_2^{(HH)}, E_2^{(HV)}, E_2^{(VV)}]^T = \mathbf{S}\mathbf{D}\boldsymbol{\sigma} + \mathbf{n}_2$$
(2)

where T denotes transposition. The columns of the 3×2 matrix \mathbf{S} contain the polarization state of each local scatterer; Elements of the 2-dimensional vector $\boldsymbol{\sigma}$ have the value of $\sigma_i e^{-j4\pi\rho/\lambda}$; Elements of the 2×2 diagonal matrix \mathbf{D} show the interferometric phase of the scatterers; \mathbf{n}_i is the noise vector. In the followings, we briefly describe basic concept of the ESPRIT algorithm. The TLS (Total Least Square) ESPRIT algorithm is employed for the experimental demonstrations described in the next section. See [6] for the details of the algorithm.

In the ESPRIT algorithm, we define the overall data vector \mathbf{x} and its correlation matrix \mathbf{R}_{xx} as,

$$\mathbf{x} = [E_1^T, E_2^T]^T$$
(3)

$$\mathbf{R}_{xx} = \langle \mathbf{x}\mathbf{x}^H \rangle$$
(4)

where H denotes complex conjugate transpose, and $\langle \rangle$ is multi-look processing or ensemble average of pixels. The number of dominant scatterers can be estimated by the

normalized eigenvalue ($\bar{\lambda}_j$) distribution of (4), which can be expressed by

$$\bar{\lambda}_1 \geq \dots \geq \bar{\lambda}_d > \bar{\lambda}_{d+1} = \bar{\lambda}_6$$
(5)

$$\bar{\lambda}_j = \lambda_j / \sum_k \lambda_k$$

where λ_k is the eigenvalue of \mathbf{R}_{xx} . When there exist only one scatterer, one dominant eigenvalue ($d=1$) appears. In the forest regions, 2 (or more) dominant eigenvalues appear in general. From this property, the number of components to be evaluated can easily be determined.

Using the eigenvectors corresponding to the dominant eigenvalues, the matrix \mathbf{D} can be estimated. Relation of the eigenvectors (e_1, \dots, e_d) and the matrices \mathbf{S}, \mathbf{D} can be written by

$$[e_1, \dots, e_d] \equiv \begin{bmatrix} F_1 \\ F_2 \end{bmatrix} = \begin{bmatrix} \mathbf{S}\mathbf{C} \\ \mathbf{S}\mathbf{D}\mathbf{C} \end{bmatrix}$$
(6)

where \mathbf{C} is a $d \times d$ non-singular matrix. From (6), the following equation can be derived:

$$F_1 \mathbf{D} F_1^H = F_2 F_1^H$$

This equation means that the diagonal elements of \mathbf{D} can be obtained by the (complex) eigenvalues of $F_2 F_1^H$ on the basis of $F_1 F_1^H$, that is:

$$|F_2 F_1^H - \lambda_i' F_1 F_1^H| = 0$$
(7)

Therefore, the interferometric phase of the i -th scatterer can be estimated by

$$\phi_i = \arg(\lambda_i')$$
(8)

When \mathbf{D} is estimated, polarization state of each local scatterer can also estimated easily [6].

This technique is also applicable to restricted dual polarization data set approximately. In this case, the measurement data vectors in (2) may be re-defined as

$$E_j = [E_j^{(pol_1)}, E_j^{(pol_2)}, 0]^T, j=1,2$$
(9)

where pol_1 and pol_2 denote the chosen set of measured channels (e.g. VV, VH). The last element (0) is a dummy component to create a null space of the signal subspace for the TLS-ESPRIT analysis.

IV. EXPERIMENTAL RESULTS

The used experimental data are L-Band scattering single-look complex (SLC) image pair of the Tien Shan test-site by the SIR-C/X-SAR system on October 8 and 9, 1994 (data takes 122.20 & 154.20). The total power image of the analyzed region is shown in Fig.3. The HH, HV, and VV data are used for the fully polarimetric analysis. Therefore, we obtain 6 eigenvalues at each image patch at the first eigenanalysis of the ESPRIT algorithm in (5). The maps of largest 2 normalized eigenvalues are shown in Figs.4 (a) and (b). As can be seen in the figures, the forest region can be clearly discriminated from the other regions using the $\bar{\lambda}_1$ map. This property is useful for forest canopy detection.

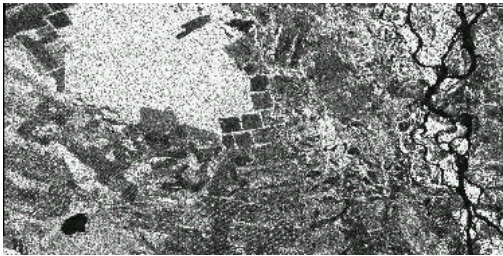


Fig3. L-Band total power image of the test area



(a) $\bar{\lambda}_1$



(b) $\bar{\lambda}_2$

Fig.4 Normalized eigenvalue maps of the TLS-ESPRIT analysis

Figure 5 shows the differential height of the dominant two phase centers in each patch. Histogram of the detected height is also shown in Fig.6 (3-pol.). The peak of the differential height locates at 10 m approximately. Almost all results are below 30 m. The real effective tree height will be higher than these values, therefore, we may say that the estimated results are acceptable.

The TLS-ESPRIT algorithm can be considered work properly for restricted dual-polarization data set. The Histograms of the estimated differential height, with HH-VV data set and VV-VH data set, are also shown in Fig.6 (2-pol.). The detection performance of the dual polarimetric analysis with HH and VV data analysis slightly deteriorates in comparison with that of the fully polarimetric estimation. The HV channel also has important information of forest canopy, although the power is small. We can still detect forest area and its differential height with only VV and HV data set. The detected number of patches decreases, however, the detected height shows similar distribution to the other results.

V. CONCLUSIONS

In this paper, we propose an alternate *Polarimetric SAR Interferometry* technique using the TLS-ESPRIT algorithm.

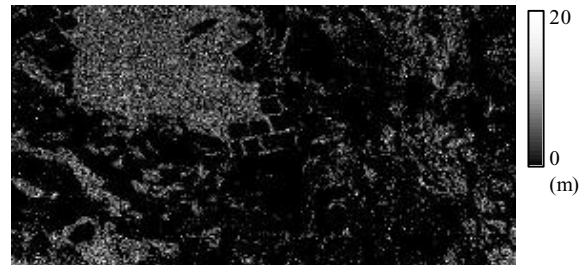


Fig.5 Differential height map by the TLS-ESPRIT algorithm

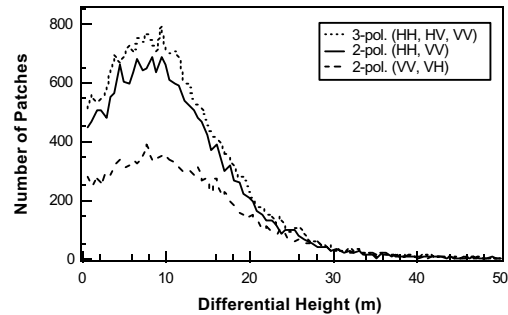


Fig.6 Histogram of the estimated differential height

The technique can work with both fully and dual polarimetric data, and detects local interferometric phase of the ground and canopy separately. Performance of the technique was demonstrated by the SIR-C/X-SAR data of the Tien Shan test site. To verify the estimation accuracy precisely, computer simulation will be required. Performance of the algorithm for single-pass data set is another theme to be considered. They will be reported in the near future.

REFERENCES

- [1] J.I.Askne, P.G.Dammert, L.M.H.Ulander, and G.Smith, "C-Band repeat-pass interferometric SAR observations of the forest," *IEEE Trans. Geosci. Remote Sensing*, vol.35, no.1, pp.25-35, Jan. 1997.
- [2] S.R.Cloude and K.P.Papathanassiou, "Polarimetric SAR interferometry," *IEEE Trans. Geosci. Remote Sensing*, vol.36, no.5, pp.1551-1565, Sept. 1998.
- [3] R.N.Treuhaft and P.R.Siqueria, "Vertical structure of vegetated land surfaces from interferometric and polarimetric radar," *Radio Science*, vol.35, no.1, pp.141-177, Jan-Feb 2000.
- [4] K.P.Papathanassiou, S.R.Cloude, A.Reigber, and W.M.Boerner, "Multi-baseline polarimetric SAR interferometry for vegetation parameter estimation," *Proc. IGRASS 2000*, VI.
- [5] S.R.Cloude and E.Pottier, "A review of target decomposition theorems in radar polarimetry," *IEEE Trans. Geosci. Remote Sensing*, vol.34, no.2, pp.498-518, Mar. 1996.
- [6] R.Roy and T.Kailath, "ESPRIT --- Estimation of signal parameters via rotational invariance techniques," *IEEE Trans. Acoust., Speech and Signal Processing*, vol.37, no.7, pp.984-995, July 1989.